JAST, Vol. 11.1, No,2, pp.

JAST
Journal of Aerospace Science and Technology

Scientific-Research Article

Output Feedback Second-Order Sliding Mode Control of Spacecraft

Ali Kasiri[1], Farhad Fani Saberi[2]*

1 - Faculty of Aerospace Engineering, Amirkabir University of Technology
2- Space Sciences and Technology Institute, Amirkabir University of Technology
* Tehran, Hafez St.

Email: *f.saberi@aut.ac.ir

This paper studies an output feedback second-order sliding mode control problem of spacecraft attitude control in the presence of the inertia tensor uncertainty and external disturbance. Mathematical modeling is presented based on spacecraft nonlinear equations of motion and quaternion parameters. Firstly, a new sliding surface based on only attitude error is selected, then the standard second-order sliding mode control approach is followed. Finally, controller stability and tracking problem are guaranteed by choosing suitable auxiliary control input. The stability is proven by using concepts of a strong Lyapunov function and Lyapunov stability theory. Numerical simulations of attitude control of spacecraft equipped with 6 PWPF thrusters are given to demonstrate the performance of the proposed controller.

***Keywords**: attitude control-second order sliding mode-finite time convergence-attitude tracking*

Introduction

Advanced space missions demand the development of effective spacecraft attitude control systems (ACS) to ensure rapid and accurate time-response to various input commands. Such a response should be achieved globally in the presence of uncertainties, internal and external disturbances, and sensor or actuator nonlinearities. A significant challenge arises when all the mentioned issues are accrued simultaneously [1]. Spacecraft attitude motion is governed by kinematic and dynamic equation. These mathematical descriptions are coupled and nonlinear. Thus, linear feedback control approaches are not suitable enough for the global controller design [2]. Standard First-order sliding-mode control (SMC) scheme has been considered as a useful technic for spacecraft-attitude control [3]. The main motivation behind SMC is the inherent robustness and simple design. Vadali [4] designed a variable-structure attitude control law based on quaternion kinematics representation. Since then, a considerable amount of researchers have investigated the application of standard conventional sliding mode control (SMC) for the attitude control of spacecraft [5,6-10]. However, chattering is a serious limitation in the standard sliding mode scheme, which can lead to hardware failure. In the simplest case, chattering can be alleviated by using mainly the boundary layer approach [11]. However, in this approach, the sliding mode is ensured within a boundary layer, but the behavior inside the boundary layer is not defined and therefore, robustness and accuracy cannot be ensured in full strength and performance deterioration is inevitable [1,12]. Higher-order sliding mode (HOSM) is also a flexible, robust and adaptive control approach, which alleviates

1 PhD. Student
2 Associate Professor (corresponding author)

chattering phenomena [13]. Additionally, HOSM control ensures that the sliding variables and their high order derivatives reach the zero (origin) in finite time [14]. Second-order sliding mode control is a specific case of HOSM control, which used to control various types of nonlinear systems [12,15]. In SMC design, the sliding surface is a linear or nonlinear combination of system states. In the case of spacecraft, body angular rate and quaternion parameters are the system's states. Thus previous researchers chose $\sigma = \omega_E + kq_E$ as sliding surface, which has proportional and derivative terms. Obviously, selection of sliding surface with this structure results the relative degree one. Designer can solve the control problem both with (i) integral second-order sliding mode (ISSM) and (ii) derivative approach. Here, to design a second-order sliding mode control with global finite-time convergence, we choose sliding surface as $\sigma = kq_E$. This sliding surface leads to deferent stability approve which is the main difference between this paper and others. This paper proceeds as follows: In Section II, the attitude kinematics and dynamics are presented and external disturbance is defined. In Section III, the second-order SMC formulation is discussed. In Section IV, the closed-loop stability is proven using the Lyapunov stability theory. Then, simulation results are shown in Section V. In the end, the paper conclusion is given in Section VI.

Spacecraft Modeling

A rigid body spacecraft attitude kinematics and dynamics, and also external disturbance are given in this section.

Kinematic Model

Quaternion parameters, due to their non-singularity computation, is the widely used parameter to represent the attitude kinematics of rigid spacecraft [16]. The kinematics equations using the quaternion parameters are given as:

$$\begin{aligned} \dot{q}_v &= \frac{1}{2}(q_4 I_{3\times 3} + q_v^{\times})\omega \\ \dot{q}_4 &= -\frac{1}{2}q_v^T\omega \end{aligned} \qquad (1)$$

where $q_v = [q_1, q_2, q_3]^T \epsilon \Re 3$ and $qq4\epsilon\epsilon\Re$ are the vector and scalar part of the unite quaternion, respectively. $I_{3\times 3}$ is the identity matrix, and $\omega = [\omega_x, \omega_y, \omega_z]^T \epsilon \Re^3$ is body angular rate. For any vector such as $m = [m_1, m_2, m_3]^T \epsilon\ \Re^3$, notation $m^{\times}$ denotes skew-symmetric matrix, which defines as follows:

$$m^{\times} = \begin{bmatrix} 0 & -m_3 & m_2 \\ m_3 & 0 & -m_1 \\ -m_2 & m_1 & 0 \end{bmatrix} \qquad (2)$$

To define the attitude kinematics and dynamics equation for tracking control problem, the relative attitude error between body frame and a desired reference frame is required to be established. The error-quaternion $q_E = [q_E^T v q_{E4}]T\epsilon\Re^3\times\Re$ which presents error between current and desired attitude is defined as follows:

$$\begin{aligned} q_{Ev} &= q_{d4}q_v - q_{dv}^{\times}q_v - q_4 q_{dv} \\ q_{e4} &= q_{dv}^T q_v + q_4 q_{dv} \end{aligned} \qquad (3)$$

where $q_E = [q_{E1}, q_{E2}, q_{E3}]^T \epsilon \Re^3$ and $q_{e4}\epsilon\Re$ are the vector and scalar part of the error-quaternion parameters. Finally, error-quaternion parameters can be updated by Eq. (4).

$$\begin{aligned} \dot{q}_{Ev} &= \frac{1}{2}(q_{E4} I_{3\times 3} + q_{Ev}^{\times})\omega_E \\ \dot{q}_{E4} &= -\frac{1}{2}q_{Ev}^T\omega_E \end{aligned} \qquad (4)$$

where ω_E is the error body angular rate between current and desired body angular velocity. In this paper we considered a rest to rest maneuver, so desired body angular velocity is zero.

Dynamic Model

The attitude dynamics of a rigid spacecraft is defined using Euler's equation and expressed as follows:

$$\dot{\omega} = J^{-1}\left(-\omega^{\times}J\omega + u(t) + d(t)\right) \qquad (5)$$

where $u(t) = [u_1, u_2, u_3]T\epsilon\Re^3$ is control input, $d(t) = [d_1, d_2, d_3]T\epsilon\Re^3$ is the external disturbances acting on the spacecraft body, and $J = diag(J_{xx}, J_{yy}, J_{zz})\epsilon\Re^{3\times 3}$ represents the spacecraft moment of inertia tensor.

Assumption 1. We assumed that quaternion parameters q (measured by sun-sensor and magnitometers) and body angular rate (measured by 3 dimensional gyroscopes) are available for feedback.

Assumption 2. The external disturbance d(t) is bounded, and the bound limit is known.

Actuator Modeling

Here, we assumed that spacecraft is equipped by 6 symmetric cold gas thrusters as shown in figure 1. Among the known pulse modulators, the pulse-width pulse-frequency (PWPF) modulators are the

most common and enjoy advantages over bang-bang control systems. PWPF modulators and on-off actuators are widely used in spacecraft control [17]. As thrusters work on on/off switching, there is a conversion from continuous desired torque control command to an on/off signal for spacecraft thrusters.

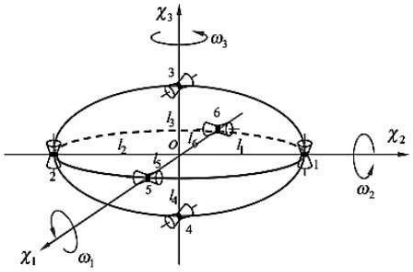

Fig. 1: six symmetric cold-gas thrusters of spacecraft

A simple model of a spacecraft equipped with PWPF thrusters is shown in Figure 2.

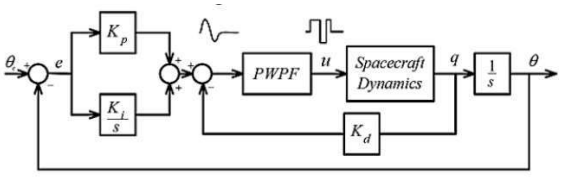

PWPF modulator is usually preferred because its operation mechanism has an almost linear input/output relationship. Also, the PWPF modulator operates in a quasi-linear mode by modulating the width of the output pulses and the distance between them simultaneously. And it can produce pulses in two directions: positive and negative pulses. A PWPF modulator mainly comprises two components: a first-order lag filter and a Schmitt trigger inside a feedback loop, as shown in Figure 3. A Schmitt trigger is an on-off relay with a dead zone and hysteresis. Four parameters should be tuned properly. These parameters are: pre-filter gain (K_m) and time constant (T_m) as well as activation (K_m) and deactivation (K_m) values of Schmitt trigger.

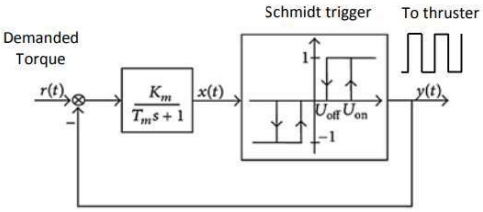

Fig. 3: Structure of PWPF modulator

Actuator specifications used in the simulation are listed in Table 1.

Table 1. PWPF Parameters

K_m	T_m	U_{on}	U_{off}
4.5	0.1	0.2	0.1

We assumed that the saturation limit of thrusters is 0.1 Nm, and the thrust force distance to the center of gravity is 1 m.

External Disturbance

To simulate the spacecraft operating environment we need to consider space disturbances. The gravity gradient is the spatial rate of change in gravitational acceleration. Which is produced because of the Nonhomogeneous mass distribution of the satellite. It's the most effective disturbance torque in 600 to 800 km. The general Equation of gravitational torque is defined as follows:

$$\vec{M} = \int \vec{r} \times \vec{a}_g \, dm \;\; ; \text{where } \vec{a}_g = -GM_E \frac{\vec{R}+\vec{r}}{|\vec{R}+\vec{r}|^3} \quad \textbf{(6)}$$

Where $\vec{r}$ and $\vec{R}$ are shown in figure 4, and M_E is math of earth.

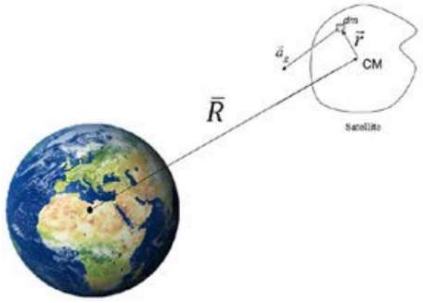

Fig. 4: Principle of Gravity Gradient Torque Scheme

Finally gravity-gradient disturbance torque calculates as [16]:

$$\begin{aligned} GG_x &= \frac{3\mu}{2r_0^3}\left(I_z - I_y\right)\sin(2\phi)\,cos^2(\theta) \\ GG_y &= \frac{3\mu}{2r_0^3}\left(I_z - I_x\right)\sin(2\theta)\cos(\phi) \\ GG_z &= \frac{3\mu}{2r_0^3}\left(I_x - I_y\right)\sin(2\theta)\sin(\phi) \end{aligned} \quad (7)$$

where μ is the standard gravitational parameter of earth, ϕ and θ are the Euler angles, and we suppose that the moving satellite is at a distance 0r from the center of mass of the earth. Quaternion parameters can transfer to the Euler angles as follows:

$$\phi = tan^{-1}\left(\frac{2(q_2q_3 + q_1q_4)}{-q_1^2 - q_2^2 + q_3^2 + q_4^2}\right)$$
$$\theta = -sin^{-1}\big(2(q_1q_3 - q_2q_4)\big) \quad (8)$$
$$\psi = tan^{-1}\left(\frac{2(q_1q_2 + q_3q_4)}{q_1^2 - q_2^2 - q_3^2 + q_4^2}\right)$$

Controller Design

Obviously, selection of sliding surface with conventional structure of $\sigma=\omega_E + kq_E$ results the relative degree one [18]. Therefore, to design a secondorder sliding mode control with global finite-time convergence, we choose $\sigma=kq_E$ as sliding surface [19]. But the main difference between this work and others is the auxiliary control input as will explained below.

$$\sigma = q_{ev} \quad (9)$$

where = $[\sigma_1, \sigma_2, \sigma_3]^T \epsilon \Re^3$.
Obviously, from Eqs. (5) and (9), the first time presence of the control input ($u(t)$) appears in the second derivative of the sliding surface (9). Therefore, selection of the sliding surface (9) causes the relative degree r = 2.
Now, it is easy to verify that the second-derivative of sliding surface yields.

$$\ddot{\sigma} = \frac{-1}{4}(q_{Ev}^T\omega_E^2 + \omega_E^{\times}(q_{E4}I_{3\times3} + q_{Ev}^{\times})\omega_E) + \frac{1}{2}(q_{E4}I_{3\times3} + q_{Ev}^{\times})\dot{\omega}_e \quad (10)$$

Using Eq. (5), yields:

$$u_{eq} = \frac{1}{2}J(q_{Ev}^T\omega_E^2 + \omega_E^{\times}G(Q)\omega_E)G^{-1}(Q) + \omega^{\times}J\omega \quad (12)$$

And total control input is as follows:

$$u_{tot} = u_{eq} + v_{disc} \quad (13)$$

where $v(t)\epsilon\Re^3$ is the auxiliary control input.

$$v_{disc} = -\mu.sign(s + \dot{s}) \quad (14)$$

Now, this controller guarantees the stability and finite time convergence.

Stability Proof

In this section, for the closed-loop system, stability proof has been discussed. The proof is discussed here based on the lyapunov theorem [20] in two steps; in the first step, it is shown that if the attitude states locate in the reign 2 and 4 of figure 5, then they will achieve to origin in finite-time without using the lyapunov. Secondly, it is shown that if the attitude states locate in the reign 2 and 4, the error in attitude states will go to the zero in finite-time by second-order sliding mode, based on the lyapunov theorem.

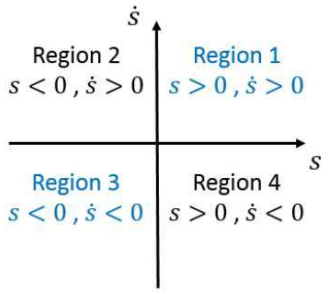

Fig. 5: $ss - s\dot{s}$ plane

Consider the lyapunov candidate as follows:

$$V(s,\dot{s}) = \frac{1}{2}s^2 + \frac{1}{2}\dot{s}^2 \quad (15)$$

It is crystal clear that $V(s,\dot{s})$ is positive definite. Following equation shows the time-derivative of V.

$$\dot{V}(s,\dot{s}) = s\dot{s} + \dot{s}\ddot{s} \quad (16)$$

Using Eqs. (11) and (12), the new form of V would be as:

$$\dot{V}(s,\dot{s}) = s\dot{s} + \frac{1}{2}G(Q)J^{-1}\dot{s}\big(-\mu.sign(s + \dot{s}) + d(t)\big) \quad (17)$$

Assumption 3. The upper bound of external disturbance is d_1, so we can claim that $|d(t)| \leq d_1$. Now, Eq. (17) can be written as follows:

$$\dot{V}(s,\dot{s}) = s\dot{s} - \dot{s}\big(\mu_1 sign(s + \dot{s})\big) + \delta \quad (18)$$

Where $\mu_1 = \mu, \delta = |Kd_1\dot{s}|$, and $K = \frac{1}{2}G(Q)J^{-1}$
Case 1. if $s\dot{s} < 0$, then we are in region 4 or 2 of the figure 5. It is obvious that in these regions $s=q_{Ev}$ will reaches to the origin, because these conditions represent a stable differential equation. Case 2. if $s\dot{s} > 0$, then we are in region 1 or 3 of the figure 5. In these cases we need to use lyapunov theorem, and the task is to prove that $\dot{V}$ is negative definite ($\dot{V} < \eta$, $whih\ \eta > 0$).

If $(s+\dot{s}) > 0$ then Eq. (18) turns to following:

$$\dot{V}(s,\dot{s}) = s\dot{s} - \dot{s}\mu_1 + \delta < -\eta \qquad (19)$$

In this case, choosing $\mu_1 > (\frac{\eta+\delta}{\dot{s}} + s)$ satisfies Eq. (19).

If $(s+\dot{s}) < 0$ then Eq. (18) turns to following:

$$\dot{V}(s,\dot{s}) = s\dot{s} + \dot{s}\mu_1 + \delta < -\eta \qquad (20)$$

In this case, choosing $\mu_1 > (\frac{\eta+\delta}{\dot{s}} + |s|)$ satisfies Eq. (20).

In both (19) and (20), Choosing $\mu_1 > (\frac{\eta+\delta}{\dot{s}} + |s|)$ guarantees the asymptotic stability of closed-loop system. Indeed, auxiliary control input plays significant role in the stability of proposed controller.

The disadvantage of proposed controller is the need for knowing about upper bound of disturbance torque (d_1) and the error of attitude (q_{Ev}) and body angular rate (ω_E).

By selecting this control signal (equation 13), the states rotate around the $s-\dot{s}$ plane to reach the origin as shown in figure 6.

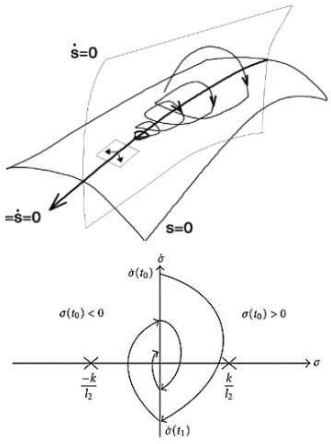

Fig. 6: schematic of $s-\dot{s}$ plane

Simulation

Simulation is conducted in the presence of external disturbance and inertia uncertainty. Specifications of the spacecraft and Orbit are given in Table 2.

Table 2. Simulation Data

Parameter	Data
Spacecraft Specification	
Mission	Earth Observation
Mmoments of inertia matrix	$J = \begin{bmatrix} 4.6 & 0 & 0 \\ 0 & 4.4 & 0 \\ 0 & 0 & 4.2 \end{bmatrix}$ [kg/m^2]
Inertia uncertainty	$\Delta J = \begin{bmatrix} \sin(0.1t) & 0 & 0 \\ 0 & \sin(0.2t) & 0 \\ 0 & 0 & \sin(0.3t) \end{bmatrix}$
Mass	100 kg
Initial attitude	$[\phi_0, \theta_0, \psi_0] = [25, 15, -5]\ deg$
Initial angular body rate	$[p_0, q_0, r_0] = [0,0,2]\ rad/sec$
desired attitude	$[\phi_d, \theta_d, \psi_d] = [0,0,0]\ deg$
Orbital Elements:	
Type	circular
Altitude	2000 km
Orbital frequency	8.2330e-04 rad/sec
Period	7.6317e+03 s
Inclination	85 deg

μ of the Eq. (14) has been chosen as 0.7 for simulation. The attitude time response history is depicted in figure 7.

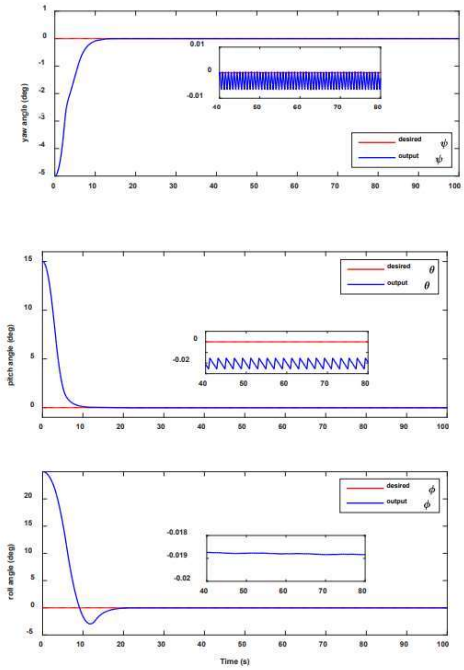

Fig. 7: Time history of attitude response

Figure 8 shows the PWPF thrusters output.

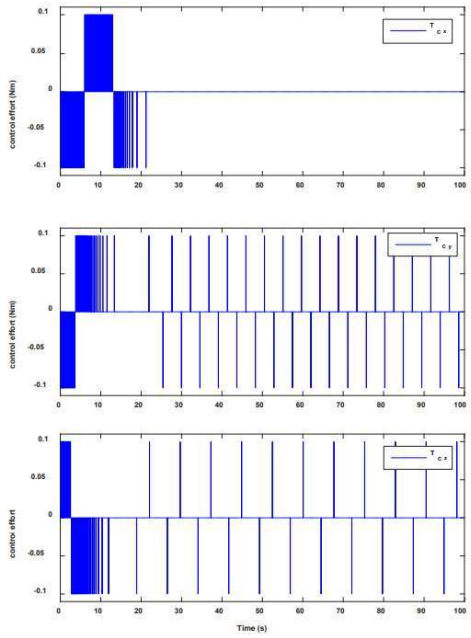

Fig. 8: Time history of thrusters output

The phase-plane of states are shown in figure 9.

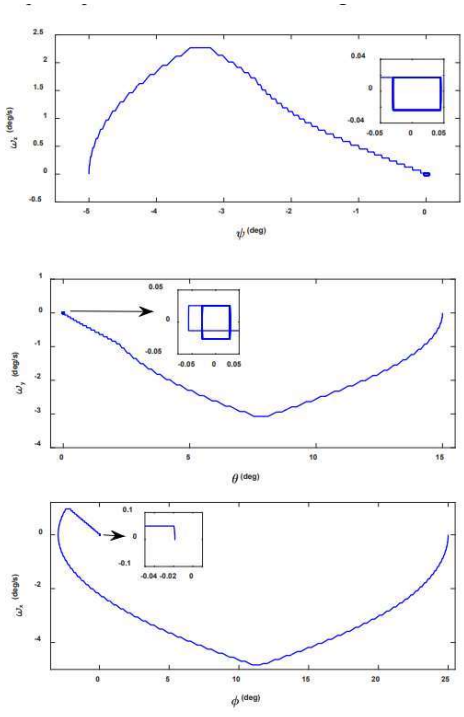

Fig. 9: phase plane

3D trajectory of Euler angles are depicted in figure 10.

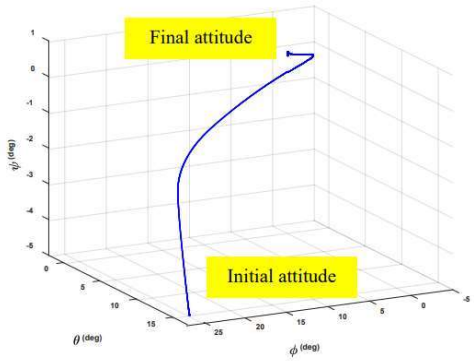

Fig. 10: Euler angles 3D trajectory

The chattering of attitude response (figure 7) is a result of PWPF mechanism and actuators' saturation limit. Figure 11 shows the attitude response in the absence of the actuator dynamics.

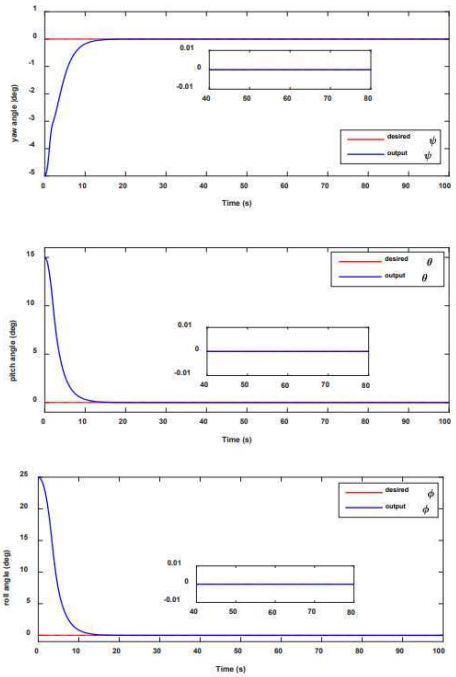

Fig. 11: Euler angles 3D trajectory

It's clear from above figure that chattering has been removed in second sliding mode controller.

Conclusion

To conclude, the second-order sliding mode attitude tracking control problem for a rigid spacecraft equipped with PWPF thrusters and subject to gravity gradient disturbance is investigated in this paper. Firstly, a sliding surface based on attitude error has been chosen (without the first time derivatives of

attitude errors). Then, the stability and robustness have been guaranteed with the use of suitable auxiliary control. Using the Lyapunov stability theory, we have proved that the error dynamics converge to near zero (origin) in finite time. This filter is suitable for use with any controller that requires knowledge of velocity and angular velocity errors. Moreover, QC3S reduces the undesirable chattering effect induced in the conventional SMC and provides very good accuracy of the tracking results. Numerical simulations on attitude control of a sample spacecraft model are also presented to demonstrate the performance of the proposed controller.

References

[1] Cai, Wenchuan, Xiaohong Liao, and David Y. Song. "Indirect robust adaptive fault-tolerant control for attitude tracking of spacecraft." Journal of Guidance, Control, and Dynamics 31, no. 5 (2008): 1456-1463. [2] DWYER III, THOMAS AW, and Hebertt Sira-Ramirez. "Variable-structure control of spacecraft attitude maneuvers." Journal of Guidance, Control, and Dynamics 11, no. 3 (1988): 262-270. [3] Pukdeboon, C., Zinober, A.S. and Thein, M.W.L., 2009. Quasi-continuous higher order sliding-mode controllers for spacecraft-attitude-tracking maneuvers. IEEE Transactions on Industrial Electronics, 57(4), pp.1436- 1444. [4] Vadali, Srinivas Rao. "Variable-structure control of spacecraft large-angle maneuvers." Journal of Guidance, Control, and Dynamics 9, no. 2 (1986): 235-239. [5] DWYER III, T.A. and Sira-Ramirez, H., 1988. Variablestructure control of spacecraft attitude maneuvers. Journal of Guidance, Control, and Dynamics, 11(3), pp.262-270. [6] Lu, Kunfeng, Yuanqing Xia, and Mengyin Fu. "Controller design for rigid spacecraft attitude tracking with actuator saturation." Information Sciences 220 (2013): 343-366. [7] Chen, Y-P., and S-C. Lo. "Sliding-mode controller design for spacecraft attitude tracking maneuvers." IEEE transactions on aerospace and electronic systems 29, no. 4 (1993): 1328-1333. [8] Lu, Kunfeng, Yuanqing Xia, Zheng Zhu, and Michael V. Basin. "Sliding mode attitude tracking of rigid spacecraft with disturbances." Journal of the Franklin Institute 349, no. 2 (2012): 413-440. [9] Yeh, F-K. "Sliding-mode adaptive attitude controller design for spacecrafts with thrusters." IET control theory & applications 4, no. 7 (2010): 1254-1264. [10] Zhu, Zheng, Yuanqing Xia, and Mengyin Fu. "Adaptive sliding mode control for attitude stabilization with actuator saturation." IEEE Transactions on Industrial Electronics 58, no. 10 (2011): 4898-4907. [11] Slotine, Jean-Jacques E., and Weiping Li. "Applied Nonlinear Control Prentice Hall." New Jersey (1991): 276-310. [12] Bartolini, Giorgio, Antonella Ferrara, and Elio Usai. "Chattering avoidance by second-order sliding mode control." IEEE Transactions on automatic control 43, no. 2 (1998): 241-246. [13] Levant, Arie. "Higher-order sliding modes, differentiation and output-feedback control." International journal of Control 76, no. 9-10 (2003): 924- 941. [14] Levant, Arie. "Universal single-input-single-output (SISO) sliding-mode controllers with finite-time convergence." IEEE transactions on Automatic Control 46, no. 9 (2001): 1447-1451. [15] Mondal, Sanjoy, and Chitralekha Mahanta. "A fast converging robust controller using adaptive second order sliding mode." ISA transactions 51, no. 6 (2012): 713- 721. [16] Sidi, Marcel J. Spacecraft dynamics and control: a practical engineering approach. Vol. 7. Cambridge university press, 1997. [17] Wang, Xinsheng, Danwei Wang, Senqiang Zhu, and Eng Kee Poh. "Fractional describing function analysis of PWPF modulator." Mathematical Problems in Engineering 2013 (2013). [18] Pukdeboon, Chutiphon, Alan SI Zinober, and May-Win L. Thein. "Quasi-continuous higher order sliding-mode controllers for spacecraft-attitude-tracking maneuvers." IEEE Transactions on Industrial Electronics 57, no. 4 (2009): 1436-1444. [19] Ma, Kemao. "Comments on “Quasi-continuous higher order sliding-mode controllers for spacecraft-attitudetracking maneuvers”." IEEE Transactions on Industrial Electronics 60, no. 7 (2012): 2771-2773. [20] Khalil, Hassan K. "Nonlinear systems." Upper Saddle River (2002).